



A Journal of the Gesellschaft Deutscher Chemiker

Angewandte Chemie

GDCh

International Edition

www.angewandte.org

Accepted Article

Title: An Artificial Heme Enzyme for Cyclopropanation Reactions

Authors: Lara Villarino, Kathryn Splan, Eswar Reddem, Cora Gutiérrez de Souza, Lur Alonso-Cotchico, Agustí Lledós, Jean-Didier Maréchal, Andy-Mark Thunnissen, and Gerard Roelfes

This manuscript has been accepted after peer review and appears as an Accepted Article online prior to editing, proofing, and formal publication of the final Version of Record (VoR). This work is currently citable by using the Digital Object Identifier (DOI) given below. The VoR will be published online in Early View as soon as possible and may be different to this Accepted Article as a result of editing. Readers should obtain the VoR from the journal website shown below when it is published to ensure accuracy of information. The authors are responsible for the content of this Accepted Article.

To be cited as: *Angew. Chem. Int. Ed.* 10.1002/anie.201802946
Angew. Chem. 10.1002/ange.201802946

Link to VoR: <http://dx.doi.org/10.1002/anie.201802946>
<http://dx.doi.org/10.1002/ange.201802946>

An Artificial Heme Enzyme for Cyclopropanation Reactions

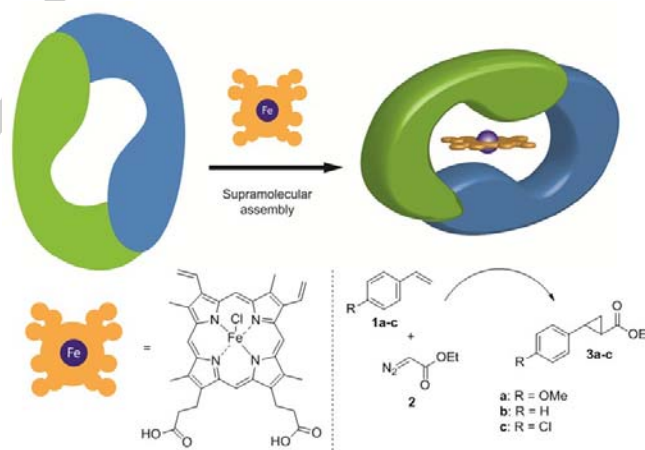
Lara Villarino,^[a] Kathryn E. Splan,^[b] Eswar Reddem,^[a] Lur Alonso-Cotchico,^[c] Cora Gutiérrez de Souza,^[a] Agustí Lledós,^[c] Jean-Didier Maréchal,^[c] Andy-Mark W. H. Thunnissen^[d] and Gerard Roelfes*^[a]

Abstract: An artificial heme enzyme was created by self-assembly from hemin and the Lactococcal multidrug resistance Regulator (LmrR). The crystal structure shows the heme bound inside the hydrophobic pore of the protein, where it appears inaccessible for substrates. Yet, good catalytic activity and moderate enantioselectivity was observed in the abiological cyclopropanation reaction. We proposed that the dynamic nature of the structure of the LmrR protein is key to the observed activity. This was supported by molecular dynamics simulations, which showed transient formation of opened conformations allowing for binding of substrates and formation of pre-catalytic structures.

Engineered heme proteins such as Cytochrome P450, Myoglobin and Cytochrome C have emerged as excellent catalysts for new-to-nature reactions,^[1, 2] including carbene transfer reactions such as cyclopropanations,^[3-7] olefinations,^[8, 9] N-H,^[10, 11] Si-H,^[12] and B-H insertion reactions.^[13] These enzymes have proven amenable to optimization by both genetic methods as well as co-factor replacement.^[14-20] A common feature of these (designed) heme enzymes is that they contain a large hydrophobic substrate binding pocket orthogonal to the plane of the heme moiety. Alternatively, significant effort has been devoted to the *de novo* design of heme proteins, particularly based on 4-helix bundles,^[21-25] antibodies or other proteins,^[26, 27] yet none of these has found application in catalysis of new-to-nature reactions. A key difference is that these artificial heme enzymes generally do not present a defined binding site suitable for binding the often hydrophobic substrates. Here, we report a novel artificial heme enzyme based on the Lactococcal multidrug resistance

Regulator (LmrR), capable of catalyzing abiological enantioselective cyclopropanation reactions. Moreover, we propose that the structural dynamics of the artificial heme enzyme are key to its catalytic activity.

LmrR is a homodimeric protein with a unique and highly dynamic structure that is key to its biological function.^[28, 29] It presents an unusually large hydrophobic and promiscuous binding pocket at the dimer interface, which has proven to be very suitable for the creation of a novel active site by anchoring of a catalytically active Cu(II) complex inside. The resulting artificial metalloenzymes have been applied successfully in enantioselective Lewis acid catalysis.^[30-33] In particular the supramolecular assembly of the artificial metalloenzyme by combination with a Cu(II)-phenanthroline complex proved powerful, giving rise to excellent enantioselectivities in the Friedel-Crafts alkylation reaction.^[34] The diversity of reactions catalysed by LmrR based artificial enzymes led us to believe that the LmrR scaffold could be extended to other catalyst types, including heme-based catalysts.



Scheme 1. Schematic representation of the assembly of the LmrR-based artificial heme enzyme and the catalyzed enantioselective cyclopropanation reaction.

The design was based on an LmrR variant that includes a C-terminal Strep tag and has two mutations in the DNA binding domain, i.e., K55D and K59Q, which facilitates expression and purification.^[31] A second mutant, LmrR_W96A, was prepared to assess the effect of the tryptophan residues in the hydrophobic

[a] Dr. L. Villarino, Dr. E. Reddem, C. Gutiérrez de Souza MSc, Prof. G. Roelfes
Stratingh Institute for Chemistry, University of Groningen
Nijenborgh 4, 9747 AG Groningen, The Netherlands
E-mail: j.g.roelfes@rug.nl

[b] Prof. K.E. Splan
Department of Chemistry, Macalester College
1600 Grand Avenue, Saint Paul, Minnesota 55105, United States

[c] L. Alonso-Cotchico MSc, Prof. A. Lledós, Prof. J.D. Maréchal
Departament de Química, Universitat Autònoma de Barcelona
Edifici C.n., 08193, Cerdanyola del Vallés, Barcelona, Spain.

[d] Dr. A. M. W. H. Thunnissen
Groningen Biomolecular Sciences and Biotechnology Institute
University of Groningen
Nijenborgh 4, 9747 AG Groningen, The Netherlands

Supporting information for this article is given via a link at the end of the document.

COMMUNICATION

pore (W96 and W96', with the prime denoting the dimer related subunit), which are known to play a role in the binding of guest molecules.^[28]

The artificial heme enzymes were created through self-assembly, by addition of iron (III) chloroporphyrin IX (*Hemin*) to the corresponding protein LmrR variant in a buffered solution (50 mM KHPO₄, 150 mM NaCl, pH 7) (scheme 1). The interaction of hemin with LmrR was examined by electronic absorption spectroscopy. The visible spectrum of hemin at pH 7.0 (Figure 1a) exhibits a broad Soret band and a weak peak c.a. 610 nm in the Q band region, which is characteristic of a π - π porphyrin dimer previously shown to predominate in aqueous hemin solutions at neutral pH.^[35, 36] Addition of LmrR results in a substantial sharpening in the Soret and Q-band regions, resulting in a spectrum that is similar to that of hemin in organic solvents.^[36] Clearly, upon addition of the protein, the dimeric porphyrin structure is disrupted and the hemin is in a monomeric form. Monitoring spectral changes as a function of added protein indicates that hemin binds to LmrR with a ratio of one hemin per dimeric protein. This stoichiometry was further confirmed via monitoring of tryptophan fluorescence quenching, which was complete upon the addition of 1 equivalent of hemin per LmrR dimer (Figure 1b). Fitting of fluorescence titration data yields a dissociation constant (K_D) of 38 ± 27 nM, indicating that the affinity of the protein for hemin is quite high, and is in fact comparable to or stronger than previously measured for other flat, planar molecules.^[28]

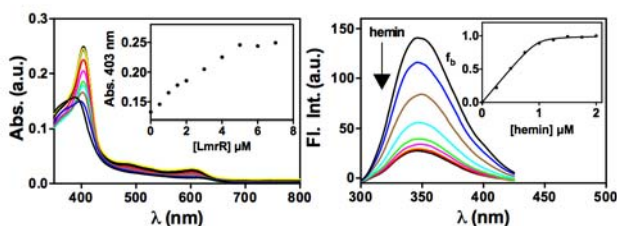


Figure 1. (a) Electronic absorption spectra upon the addition of LmrR to 5 μ M hemin. Inset: Changes in absorption values as a function of protein concentration. Buffer: 50 mM phosphate buffer/150 mM NaCl, pH 7.0. (b) Fluorescence spectra upon the addition of hemin to 1 μ M LmrR dimer. Inset: Fraction of LmrR bound to hemin as a function of added hemin concentration. Buffer: 50 mM phosphate buffer/150 mM NaCl, pH 7.0.

In contrast, UV/vis titration of hemin with LmrR_W96A results in a loss of spectral intensity, but no substantial change in spectral line shape, likely owing to non-specific binding on the protein surface (Figure S4). These results clearly show that W96/W96' play a key role in the interaction of hemin with LmrR that leads to a monomeric hemin structure, and indicate that hemin lies either partly or entirely within the hydrophobic pocket.

Hemin:LmrR stoichiometry and the importance of W96/W96' in complex formation are further supported by the crystal structure of LmrR co-crystallized with hemin (Figure 2, S6). Crystals diffracting to sufficiently high resolution could be obtained only for

an LmrR that had the K55 and K59 residues reintroduced. The overall conformation of LmrR is similar to that observed in previously published drug-bound complexes.^[28] Electron density in between the indole rings of the central W96/W96' pair is attributed to the presence of the bound heme. Clear density is observed only for the porphyrin ring, owing in part to a crystallographic 2-fold axis, but also to a lack of specific stabilizing interactions with the polar peripheral heme substituents. The heme, lacking the axial chloride ligand, was modelled in the LmrR crystal structure with four alternate binding modes, differing by rotations around a central axis perpendicular to the plane of the heme, and by a flip of the heme due the crystallographic 2-fold symmetry (Figure S6). In all binding modes, the heme-iron is shielded at either side of the heme by the indole ring of W96 and W96' and lies at an average distance of ~ 4 Å from the carbon atoms, suggesting cation- π interactions. Further stabilization is provided by van der Waals contacts with hydrophobic residues in the vicinity of the central tryptophan pair, i.e., M8, A11 and V15 (and their equivalents from the dimer mate). This structure is unlikely to allow for catalysis, as the catalytic iron is fully shielded and cannot be accessed by substrates. However, the crystal structure already suggests considerable dynamics in the binding of the heme, which may include catalytically viable conformations. This was supported by MD simulations (vide infra).

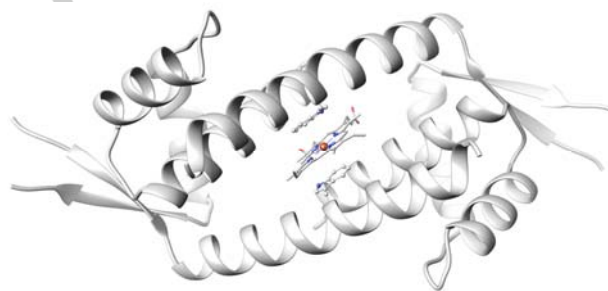


Figure 2. Crystal structure of LmrR-co-heme (PDB 6FUU). The protein crystallized in a tetragonal crystal form with one polypeptide chain occupying the asymmetric unit; the functional dimer (here shown in cartoon representation) being formed by a crystallographic dyad. In the electron density maps, the polypeptide chain is well defined, except for the tip region of the β -wing (residues 70–73) and the N- and C-termini (residues 1–4 and 109–131, including the C-terminal strep-tag). These regions show a high degree of disorder and were excluded from the final model. The heme is stacked in between the side chains of W96/W96' (for clarity only one of the alternate heme binding orientations is shown).

The potential of the artificial heme enzymes in catalysis was examined in the cyclopropanation of *o*-methoxystyrene (**1a**) with ethyldiazoacetate (EDA, **2**) under anaerobic conditions as the benchmark reaction (Tables 1, S4). In the absence of LmrR, the reaction was sluggish and diethyl fumarate (**4**), which results from the dimerization of EDA, was found as the major product (entry 1). The artificial heme enzyme (LmrR-co-heme) was assembled *in situ* by addition of 1 mol% of hemin to a slight excess (1.1 equiv) of LmrR in previously deoxygenated 50 mM KPi buffer pH 8.0. The LmrR-co-heme catalyzed reaction requires addition of sodium

COMMUNICATION

dithionate as reductant to generate the Fe(II)-heme, which is the active complex required for carbene generation. The reaction was started by addition of 30 mM of **1a** and 10 mM of **2**. After 18 h at 4°C, the *trans* isomer of the cyclopropanation product **3a** (*trans/cis*=92:8) was obtained as the major product in 25% yield, which corresponds to a total turnover number (TTN) of 247, and with an *ee* of 17%. (entry 2). The only detectable side product was diethyl fumate (**4**), with 28 turnovers. These results clearly show the acceleration and chemoselectivity due to the LmrR scaffold compared to the reactions catalyzed by hemin alone, under the same conditions.

Table 1. Results of cyclopropanation reaction of styrene derivatives **1a-c** with EDA (**2**) catalyzed by LmrR-heme.^[a]

entry	LmrR	1 ^[c]	3	Yield %	TTN	3/4	ee % ^[b]
1	-	1a	3a	5 ± 2	51	0.8	-
2	LmrR	1a	3a	25 ± 11	247	11	17 ± 5
3	LmrR_F93A	1a	3a	23 ± 2	232	9	11 ± 1
4	LmrR_D100A	1a	3a	38 ± 8	375	20	24 ± 5
5	LmrR_W96A	1a	3a	28 ± 13	276	8	< 5
6	LmrR_V15A	1a	3a	1.5 ± 0.5	15	3	17 ± 1
7	LmrR_M8A	1a	3a	36 ± 13	359	15	44 ± 12
8 ^[c]	-	1a	3a	5 ± 2	51	0.8	-
9 ^[c]	LmrR_M8A	1a	3a	45 ± 9	449	6	51 ± 14
10 ^[c]	-	1b	3b	6 ± 0	59	n.d.	-
11 ^[c]	LmrR_M8A	1b	3b	39 ± 13	391	n.d.	38 ± 5 ^[d]
12 ^[c]	-	1c	3c	1 ± 0	12	0.2	-
13 ^[c]	LmrR_M8A	1c	3c	35 ± 13	351	3	25 ± 5

[a] Conditions: **1** (30 mM), **2** (10 mM), hemin (1 mol%; 10 μM), LmrR_X (1.1 mol%; 11 μM) in 50 mM phosphate buffer (pH 8.0), under Ar, at 4°C for 18h; Results are the average of at least two independent experiments, both carried out in duplicate. [b] of the *trans* product; *trans/cis* > 85:15. [c] pH 7.0. [d] of the 1*R*, 2*R* enantiomer.^[37]

The role of the protein scaffold was explored further by mutagenesis of residues in and around the hydrophobic pore. In addition to W96 (*vide supra*), residues M8, V15, F93, and D100 were mutated to alanine (see ESI). With the exception of V15A, all mutants showed significant protein enhanced catalytic activity that was comparable or greater than LmrR itself (entry 3-7). Surprisingly, this was also the case for LmrR_W96A, albeit with a complete loss of enantioselectivity. We attribute this to hemin-LmrR_W96A association away from the hydrophobic pore, which may result in assemblies that are catalytically active but lack the defined chiral interactions to induce enantioselectivity. A

significant increase in activity was observed in case of the mutants D100A and M8A, with the latter also giving rise to the highest enantioselectivity, that is, 44% *ee* (entry 7).

Further optimization of the reactions conditions was performed with this mutant (Tables S5-6). It was found that a threefold excess of styrene over EDA and pH 7 were the optimal conditions in terms of activity and selectivity (entry 9)

The activity of LmrR_M8A-heme was compared for substrates **1a-c**. (entries 8-13). In all cases, the artificial heme enzyme significantly outperformed the free hemin cofactor. The enantioselectivity observed ranged from 25% *ee* in the case of **3c** (entry 13) to 51% *ee* in the case of **3a** (entry 9).

The observed catalytic activity and enantioselectivity are difficult to rationalize based on the crystal structure, which shows the catalytic iron center sandwiched between the two tryptophan residues where it is inaccessible for the substrates. To gain more insight into the origin of the catalytic activity, computational studies were performed.

Calculations focused on determining the conformational rearrangement required for LmrR-heme to allow substrate binding and the reaction to take place. Local and global rearrangements of the protein were assessed for the binding of the heme as well as in presence of the substrates by combining protein-Ligand Docking, Quantum Mechanics calculations and large scale Molecular Dynamics simulations.

Protein-ligand dockings of both the heme (**5**) and its adduct with the carbene intermediate (**6**) (Figure S6) were carried out on LmrR, starting from the LmrR-heme crystal structure. Local rearrangements were assessed by introducing rotameric flexibility for all the amino acids at the dimer interface. For **5** and **6**, four binding poses with good predicted affinity (ChemScore values higher than 50 units) were found for both cases (Table S3). They correspond to different orientations of the heme group as a result of rotations around the axis perpendicular to the average plane of the heme passing through the metal. The best docking solutions of LmrR-**5** show the heme sandwiched between W96/W96', similar to the crystal structure. However, in the case of the carbene complex (LmrR-**6**), some low energy solutions present W96' rotated towards the solvent, thus providing space to accommodate the co-substrate (Figure S1). To assess the structural rearrangement of LmrR upon heme binding, the four predicted structures of LmrR-**5** and LmrR-**6** were submitted to 100ns MD simulations.

Cluster analysis shows a high stability of the LmrR-heme complex (Figure S8), with W96 and W96' generating a hydrophobic patch that sandwiches the heme. Some of the most populated clusters of the LmrR-**5** system (clusters 1 and 3-6) show high similarity with the crystal structure, with the iron atom inaccessible to solvent (Figure 3a). On the other hand, clusters 0 and 2 (see SI for details), show changes in the orientation of the α helix containing W96' (α 4) and a flip of the W96' indole towards the outside of the pore (Figures 3b, S10). These predicted

COMMUNICATION

conformational changes are in agreement with previous reports that flexibility in the orientation of $\alpha 4$ is a major contributor to the ability of LmrR to structurally adapt to different drug molecules.^[29] These changes in the protein structure are accompanied by a significant displacement of the heme towards the solvent. The result is an opened conformation that has significant free space on the axial face of the heme group. This appears of key importance to catalysis, since the iron site becomes accessible to bind the carbene, which allows the reaction occur.

MD simulations of the LmrR-heme-carbene complex (LmrR-**6**) show that this opened conformation is indeed capable of accommodating the carbene moiety. The simulations further underline the importance of W96' in controlling the accessibility of the heme-carbene complex. With W96' pointing towards the hydrophobic core, the heme-carbene is directed towards the solvent, where it will be accessible for the styrene co-substrate (Figure 3c). Rotation of W96' to the outside of the pore causes the heme-carbene (**6**) to remain at the dimer interface (Figure 3d, S8).

Finally, the effect of the second substrate (styrene) was studied. First, the transition state geometry that leads to the generation of the 1R,2R cyclopropane was obtained by QM calculations (Figure S7) and then subjected to the same analysis as before (Table S3). The majority of the structures (clusters 0, 2 and 3) correspond LmrR with a broader dimer interface where the two helices containing the W96/W96' residues appear further separated and are thus capable of accommodating the catalytic complex (Figure 3e). W96' appears to be involved in stabilizing the TS structure through π -stacking with the phenyl group of the styrene.

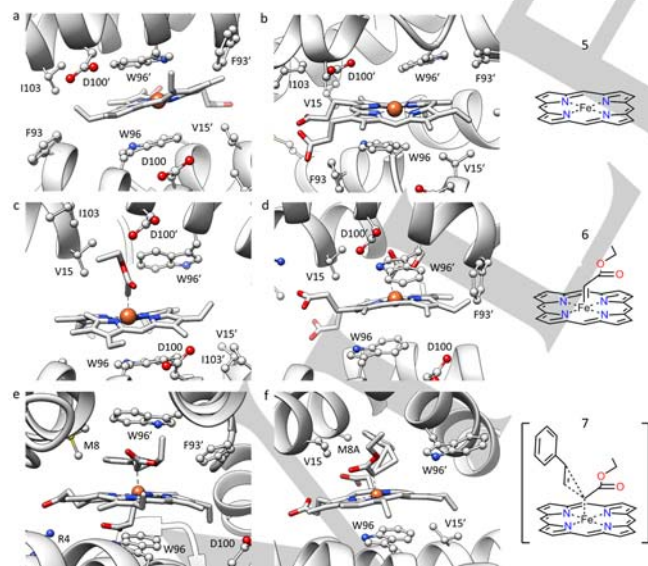


Figure 3. Representative structures resulting from MD simulations of: the LmrR-heme system ((a) cluster 3, RMSD with crystal 1.634 Å and (b) cluster 2 RMSD with crystal 2.471 Å, 400 ns MD simulation), the LmrR-heme-carbene system ((c) cluster 0, RMSD with crystal of 0.548 Å and (d) cluster 2, RMSD with crystal of 1.000 Å, 400ns MD simulation) and the cyclopropanation transition state ((e) into LmrR, (f) into LmrR_M8A, 100ns MD simulation).

Since the M8A mutant showed the best results in catalysis, the dynamic behaviour of this artificial metalloenzyme was also studied. For consistency, all the simulations were carried out in the same conditions as before. The system resulting from the docking of the heme linked to the TS structure for the 1R,2R enantiomeric product into the LmrR protein was selected as starting point for a 100ns MD simulation, which suggests that the effect of this mutation is mainly steric: the aromatic moiety of the styrene now occupies the free space resulting from the change of the large methionine into the much smaller alanine. Also, W96' is flipped towards the solvent and thus contributes to binding of the TS structure into the dimer interface (Figure 3f).

The combined results demonstrate unequivocally that the cyclopropanation reaction occurs in the hydrophobic pocket of LmrR. Initially, this is counterintuitive: heme enzymes such as P450 usually present a large hydrophobic cavity for binding substrates whereas, in contrast, upon binding of hemin, the pocket of LmrR is fully occupied. Yet, the artificial enzyme exhibits good activity and shows enantioselectivity in catalysis. This is attributed to the dynamic nature of the LmrR based artificial heme enzyme involving substantial geometric rearrangement of the heme environment to allow for binding of the substrates and their interaction with the heme. Indeed, the MD simulations show that the LmrR-heme complex undergoes significant conformational changes, giving rise to transient open conformations that make it possible to reach a pre-catalytic state, allowing the reaction to proceed.

In conclusion, we have created an artificial heme enzyme based on the protein LmrR, which shows good activity and moderate enantioselectivity in an abiological reaction, that is, the catalytic cyclopropanation of styrenes. This represents the first example of organometallic catalysis with an LmrR based artificial metalloenzyme and thus illustrates the versatility of LmrR as a scaffold for artificial metalloenzymes design. A key finding is that enzyme is active despite the fact that the crystal structure shows a tightly bound heme that appears inaccessible to substrates. It is proposed that the artificial enzyme can open up to allow formation of precatalytic structures, as a result of the dynamics of the protein-heme assembly. Molecular dynamics studies add support to this hypothesis. This work suggests that dynamics has to be taken into account in the design of artificial enzymes and may be key to achieving catalytic activity.

Experimental Section

Representative procedure for the catalytic cyclopropanation: The following final concentrations were typically used in catalysis: 30 mM styrene, 10 mM EDA, 10 mM Na₂S₂O₄, 10 μ M hemin and 11 μ M LmrR in a final volume of 720 μ L. 50 mM potassium phosphate buffer and 80 μ L of a 100 mM Na₂S₂O₄ solution were combined in a sealed vial equipped with a stir bar and degassed by bubbling argon through the mixture for 10 min. Next, a buffered LmrR solution was added carefully. Degassing was continued by flushing Ar without bubbling. In a separate vial, 80 μ L of a solution of hemin (100 μ M, pre-dissolved in buffer/DMSO, final fraction of

COMMUNICATION

DMSO 5% v/v) was deoxygenated by bubbling argon through the solution for at least 10 min, and added into the reaction via cannula. After incubation for 30 min, fresh stock solutions of **1a** (20 μ L, 1.2 M in DMSO) and **2** (20 μ L, 0.4 M in DMSO) were added and the reaction was stirred at 4°C for 18h under a positive argon pressure. The reactions were analyzed by adding 100 μ L of internal standard (2-methylanisole, 1 mM in EtOAc) to the reaction mixture, followed by extraction with ethyl acetate (800 μ L) after vortex for 1 min. The organic layers were dried over Na_2SO_4 while vortexing for 1 min. Yields, enantio- and stereoselectivity were determined by HPLC or GC-FID.

Acknowledgements

The authors thank Dr. I. Drienovská and S. Chordia for help and advice on molecular biology, the European Synchrotron Radiation Facility (ESRF) for provision of synchrotron radiation facilities and the beam-line staff of MASSIF-3 for their assistance. Financial support from the Netherlands Organization for Scientific Research (NWO, vici grant 724.013.003), the European Research Council (ERC starting grant 280010), the Spanish MINECO (CTQ2017-87889-P), the Ministry of Education, Culture, and Science (Gravitation program no. 024.001.035), a postdoctoral grant from the Xunta de Galicia (I2C Plan, to L.V.) and a PhD grant from the Generalitat de Catalunya (to L.A.C.) is gratefully acknowledged.

Keywords: artificial metalloenzymes • heme • biocatalysis • carbene • enzyme design

- [1] C. K. Prier, F. H. Arnold, *J. Am. Chem. Soc.* **2015**, *137*, 13992-14006.
- [2] O. F. Brandenburg, R. Fasan, F. H. Arnold, *Curr. Opin. Biotechnol.* **2017**, *47*, 102-111.
- [3] P. S. Coelho, E. M. Brustad, A. Kannan, F. H. Arnold, *Science* **2013**, *339*, 307-310.
- [4] P. S. Coelho, Z. J. Wang, M. E. Ener, S. A. Baril, A. Kannan, F. H. Arnold, E. M. Brustad, *Nat. Chem. Biol.* **2013**, *9*, 485-487.
- [5] M. Bordeaux, V. Tyagi, R. Fasan, *Angew. Chem. Int. Ed.* **2015**, *54*, 1744-1748; *Angew. Chem.* **2015**, *127*, 1764-1768.
- [6] J. G. Gober, A. E. Rydeen, E. J. Gibson-O'Grady, J. B. Leuthaeuser, J. S. Fetrow, E. M. Brustad, *ChemBioChem* **2016**, *17*, 394-397.
- [7] A. Tinoco, V. Steck, V. Tyagi, R. Fasan, *J. Am. Chem. Soc.* **2017**, *139*, 5293-5296.
- [8] V. Tyagi, R. Fasan, *Angew. Chem. Int. Ed.* **2016**, *55*, 2512-2516; *Angew. Chem.* **2016**, *128*, 2558-2562.
- [9] M. J. Weissenborn, S. A. Löw, N. Borlinghaus, M. Kuhn, S. Kummer, F. Rami, B. Plietker, B. Hauer, *ChemCatChem* **2016**, *8*, 1636-1640.
- [10] Z. J. Wang, N. E. Peck, H. Renata, F. H. Arnold, *Chem. Sci.* **2014**, *5*, 598-601.
- [11] G. Sreenilayam, R. Fasan, *Chem. Commun.* **2015**, *51*, 1532-1534.
- [12] S. B. J. Kan, R. D. Lewis, K. Chen, F. H. Arnold, *Science* **2016**, *354*, 1048-1051.
- [13] S. B. J. Kan, X. Huang, Y. Gumulya, K. Chen, F. H. Arnold, *Nature* **2017**, *552*, 132-136.
- [14] H. M. Key, P. Dydio, D. S. Clark, J. F. Hartwig, *Nature* **2016**, *534*, 534-537.
- [15] H. M. Key, P. Dydio, Z. Liu, J. Y. - Rha, A. Nazarenko, V. Seyedkazemi, D. S. Clark, J. F. Hartwig, *ACS Centr. Sci.* **2017**, *3*, 302-308.
- [16] G. Sreenilayam, E. J. Moore, V. Steck, R. Fasan, *Adv. Synth. Catal.* **2017**, *359*, 2076-2089.
- [17] K. Ohora, H. Meichin, L. Zhao, M. W. Wolf, A. Nakayama, J. Hasegawa, N. Lehnert, T. Hayashi, *J. Am. Chem. Soc.* **2017**, *139*, 17265-17268.
- [18] G. Sreenilayam, E. J. Moore, V. Steck, R. Fasan, *ACS Catal.* **2017**, *7*, 7629-7633.
- [19] T. Yonetani, T. Asakura, *J. Biol. Chem.* **1969**, *244*, 4580-8.
- [20] T. Hayashi, H. Dejima, T. Matsuo, H. Sato, D. Murata, Y. Hisaeda, *J. Am. Chem. Soc.* **2002**, *124*, 11226-11227.
- [21] C. Choma, J. Lear, M. Nelson, P. Dutton, D. Robertson, W. DeGrado, *J. Am. Chem. Soc.* **1994**, *116*, 856-865.
- [22] C. Reedy, B. Gibney, *Chem. Rev.* **2004**, *104*, 617-649.
- [23] I. V. Korendovych, A. Senes, Y. H. Kim, J. D. Lear, H. C. Fry, M. J. Therien, J. K. Blasie, F. A. Walker, W. F. DeGrado, *J. Am. Chem. Soc.* **2010**, *132*, 15516-15518.
- [24] Y. Lin, E. B. Sawyer, J. Wang, *Chem. Asian J.* **2013**, *8*, 2534-2544.
- [25] C. C. Moser, M. M. Sheehan, N. M. Ennist, G. Kodali, C. Bialas, M. T. Englander, B. M. Discher, P. L. Dutton, *Methods Enzym.* **2016**, *580*, 365-388.
- [26] J. -P. Mahy, J. -D. Maréchal, R. Ricoux, *Chem. Commun.* **2015**, *51*, 2476-2494.
- [27] F. Schwizer, Y. Okamoto, T. Heinisch, Y. Gu, M. M. Pellizzoni, V. Lebrun, R. Reuter, V. Köhler, J. C. Lewis, T. R. Ward, *Chem. Rev.* **2018**, *118*, 142-231.
- [28] P. K. Madoori, H. Agustiandari, A. J. M. Driessen, A. M. W. H. Thunnissen, *EMBO J.* **2009**, *28*, 156-166.
- [29] K. Takeuchi, Y. Tokunaga, M. Imai, H. Takahashi, I. Shimada, *Sci. Rep.* **2014**, *4*, 6922.
- [30] I. Drienovská, A. Rioz-Martínez, A. Draksharapu, G. Roelfes, *Chem. Sci.* **2015**, *6*, 770-776.
- [31] J. Bos, A. García-Herraiz, G. Roelfes, *Chem. Sci.* **2013**, *4*, 3578-3582.
- [32] I. Drienovská, L. Alonso-Cotchico, P. Vidossich, A. Lledos, J. Maréchal, G. Roelfes, *Chem. Sci.* **2017**, *8*, 7228-7235.
- [33] J. Bos, F. Fusetti, A. J. M. Driessen, G. Roelfes, *Angew. Chem. Int. Ed.* **2012**, *51*, 7472-7475; *Angew. Chem.* **2012**, *124*, 7590-7593.
- [34] J. Bos, W. R. Browne, A. J. M. Driessen, G. Roelfes, *J. Am. Chem. Soc.* **2015**, *137*, 9796-9799.
- [35] K. A. de Villiers, C. H. Kaschula, T. J. Egan, H. M. Marques, *J. Biol. Inorg. Chem.* **2007**, *12*, 101-117.
- [36] C. Asher, K. A. de Villiers, T. J. Egan, *Inorg. Chem.* **2009**, *48*, 7994-8003.
- [37] A. Abu-Elfotouh, K. Phomkeona, K. Shibatomi, S. Iwasa, *Angew. Chem. Int. Ed.* **2010**, *49*, 8439-8443; *Angew. Chem.* **2010**, *122*, 8617-8621.